

# Simulation of Electric Machinery and Power Electronics Interfacing Using MATLAB/SIMULINK

Daniel Logue, Philip. T. Krein

Department of Electrical and Computer Engineering  
University of Illinois at Urbana-Champaign  
Urbana, Illinois 61801-2918 USA

**Abstract**—This paper introduces power electronic and electric machines toolboxes based on the MATLAB/SIMULINK<sup>1</sup> simulation package. Simulation components include dc-dc converters, power-factor-correction rectifiers, field-oriented and direct torque control methods for electric drives, induction machines, dc machines, synchronous machines, and more complete systems. Switching and averaged power electronic models are included, as well as dynamic and steady-state machine models. The toolboxes make possible the straightforward construction and simulation of complex dynamic systems involving power electronic components and machines.

## I. INTRODUCTION

The subject of this paper is the simulation of power electronic systems and electric machines using the Matlab/Simulink simulation package. Matlab is primarily a computation engine with a full suite of mathematical functions, integration routines and numerical solvers. Simulink is a graphical interface that provides a straightforward way to use Matlab's functionality for simulation of dynamic systems [1]. Simulink models are created by constructing block diagrams similar to the well known block diagrams of control theory.

These tools have been used in many instances for the simulation of power electronic components and electric machines, but prior examples usually involve the construction of a program for a specific application [2-6]. In other instances, libraries of Simulink components have been introduced [7,8]. The toolboxes introduced here are of the latter case. They are for the design and simulation of general power electronic and machines problems. This high-level package does not require the construction of power electronic systems such as dc-dc converters, although lower level construction capability is provided. Several converters are already present in the package in forms that include switching models with and without parasitic elements, averaged models with and without parasitic elements, and steady-state models.

Each of the power electronic or machine components represent subsystems within the simulation environment. These blocks have been developed so they can be interconnected in a consistent and simple manner for the construction of complex systems. High-level control

techniques are constructed using block diagrams exactly as in typical control theory. The composition of systems of electronic components is slightly different, requiring feedforward of an independent variable such as voltage, and feedback of an independent variable such as current. This distinction arises from the desire to model the power components closely while avoiding details of the integrated circuits that make up the control processes.

The subsystems are masked, meaning that the user interface displays only the complete subsystem and user prompts gather parameters for the entire subsystem. Relevant parameters can be set by double-clicking a mouse or pointer on each subsystem block, then entering the appropriate values in the resulting dialog window. The underlying subsystem structure is clear enough that modification is simple, and the parameters can be made dependent on other system variables or dynamically adjusted during simulation if necessary.

Modeling of machines and power electronic systems using Simulink is considered in Section II. Section III explains the methodology used for general block interconnection and Section IV presents a brief overview of the blocksets. Section V describes the construction and simulation of several example systems. Note that these systems are not necessarily chosen for their practicality, but rather for their usefulness in demonstrating the simulation program.

## II. COMPONENT MODELING

Simulink requires that the component descriptions be integro-differential equations, perhaps with algebraic constraints. The package bundles the describing equations, and uses the Matlab routines for time integration of the corresponding ordinary differential equations [1]. The equations for a typical machine are in the form [9]

$$\begin{aligned}\dot{\mathbf{x}} &= \mathbf{f}(\mathbf{x}, \mathbf{u}, t) \\ \mathbf{y} &= \mathbf{g}(\mathbf{x}, \mathbf{u})\end{aligned}\tag{1}$$

where the right-hand-side is a function of the state vector  $\mathbf{x}$ , the input vector  $\mathbf{u}$ , and possibly time  $t$ . The right-hand-side (rhs) is continuous in the state vector  $\mathbf{x}$  and time  $t$ , but if connected to a power electronic converter, not necessarily in  $\mathbf{u}$ . The equations can be nonlinear. The vector of output variables is denoted by  $\mathbf{y}$ .

The describing state equation for a power electronic component is given by a network equation [10]

<sup>1</sup>Matlab and Simulink are registered trademarks of The Mathworks, Inc.

$$\dot{\mathbf{x}} = \mathbf{f}(\mathbf{x}, \mathbf{u}, \mathbf{q}, t) \quad (2)$$

where  $\mathbf{q} = [q_1 \ q_2 \ \dots]^T$  is a vector of switching functions each of which take on values of either 0 or 1. The output vector is usually the same as that in (1). Since  $q_j$  is either 0 or 1, the rhs of (2) is discontinuous by definition. An autonomous power electronic component with only two switches and one input can be described by

$$\dot{\mathbf{x}} = q_1 \bar{q}_2 \mathbf{f}_1(\mathbf{x}, \mathbf{u}) + \bar{q}_1 q_2 \mathbf{f}_2(\mathbf{x}, \mathbf{u}) + \bar{q}_1 \bar{q}_2 \mathbf{f}_3(\mathbf{x}, \mathbf{u}) \quad (3)$$

where the over-bar indicates complement. The last term on the rhs of (3) describes the system in discontinuous conduction mode, and is not needed in many cases.

The equations for the power electronic components are implemented in the form of (3) where the switching functions are generated by either logic functions or the conventional triangle-comparison pulse-width modulation (PWM) method. Because the equations contain discontinuities, a variable step solver may not be appropriate, although sometimes variable-step or stiff solvers will function satisfactorily. Systems that implement feedback based on discontinuous variables usually cause a variable-step solver to fail. In these cases, one must rely on a fixed-step solver, even though the short time step usually lengthens the necessary simulation time.

It is important to realize that the block models for the power electronic components are behavioral based [11-13]. This means that the low level operation of the switching elements and similar devices are ignored, the switch is idealized, and takes on a binary representation of either on or off. Switching losses can be estimated based on higher-level functions such as switching frequency, current levels, and generalized switching trajectories. The control components are modeled in terms of ideal integrators, summing blocks, etc., for controller composition.

#### A. Dc Machine Modeling

The modeling of the separately excited dc machine in this environment is taken up in this section. The armature and field equations are

$$L_a \frac{di_a}{dt} = v_a - R_a i_a - L_{af} i_f \omega \quad (4)$$

$$L_f \frac{di_f}{dt} = v_f - R_f i_f \quad (5)$$

where  $L_a$  and  $L_f$  are the armature and field winding self-inductances, respectively. The armature and field winding resistances are  $R_a$  and  $R_f$  respectively. The mutual inductance between the armature and field is  $L_{af}$ , and  $\omega$  is the shaft speed in rad/s. The armature input voltage is  $v_a$ , and the field voltage is  $v_f$ . The developed electric torque is given by

$$T_e = L_{af} i_f i_a \quad (6)$$

The differential equation describing the shaft speed is

$$\frac{d\omega}{dt} = \frac{1}{J} (T_e - T_{load}) \quad (7)$$

where  $J$  is the rotational inertia of the machine and load. Notice that effects from remanent magnetism, commutation, and friction have been neglected for simplicity in this instance. The actual models within the machines toolbox include these effects.

The block diagram for the separately excited dc machine is shown in the necessary form in Fig. 1. Inputs include the armature and field voltages, and the load torque. Outputs include the winding currents, the developed torque, and the shaft speed. As shown, the block diagram is built directly from the machine equations.

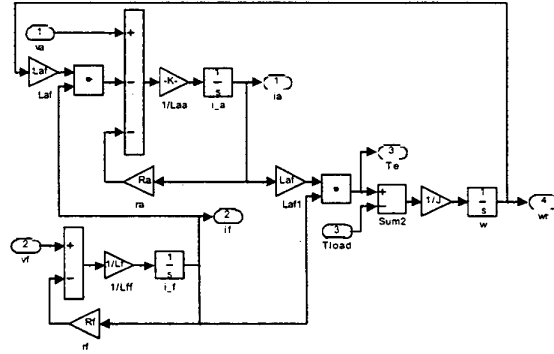


Fig. 1 Separately excited dc machine Simulink block diagram.

#### B. Buck Converter Modeling

The buck converter with ideal switching devices will be considered here to convey the way in which these types of systems are modeled. The state equations corresponding to the converter in continuous conduction mode are

$$\begin{aligned} \frac{di_L}{dt} &= \frac{1}{L} (q_1 V_{in} - v_c) \\ \frac{dv_c}{dt} &= \frac{1}{C} \left( i_L - \frac{v_c}{R_L} \right) \end{aligned} \quad (8)$$

where  $i_L$  is the inductor current,  $v_c$  is the output capacitor voltage,  $L$  is the inductance,  $C$  is the output capacitance,  $R_L$  is the load resistance, and  $q_1$  is the switching function corresponding to the controlled switch. These equations are implemented in Simulink as shown in Fig. 2 where a PWM block has been added to drive the system. Only the  $q_1$  output of the PWM block is utilized, because the equations (8) do not require  $q_2$ . The rhs of these equations are modeled using multipliers, summing blocks, and gain blocks, and

subsequently fed into two integrators to obtain the states  $i_L$  and  $v_C$ . The converter input current is supplied as a system output, while the output current is an input. This will be discussed in more detail in the next section.

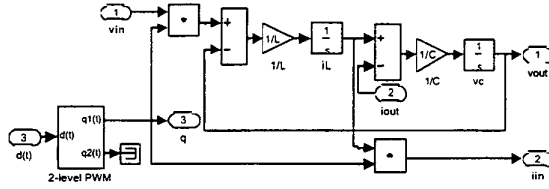


Fig. 2 Block diagram of simple buck converter.

### III. SUBSYSTEM INTERCONNECTION

The components that make up the block libraries must be constructed so the interconnection of blocks is consistent and straightforward. In most cases, each component block has independent variables for inputs and delivers outputs which act as independent inputs to subsequent blocks. For instance, consider a simple resistor with terminal conditions defined by Ohm's law. The input to a resistor block can be either its terminal voltage or current. If the input is voltage, the resistor block will return its terminal current.

The basic subsystem structure is displayed in Fig. 3 where the vectors  $u_1$ ,  $u_2$ ,  $v$ , and  $p$  are inputs, and  $y_1$  and  $y_2$  are outputs. The vector  $v$  provides independent inputs to the subsystem, while  $p$  dynamically adjusts parameter values. The partition of the input vector  $u=[u_1 \ u_2]^T$  and output vector  $y=[y_1 \ y_2]^T$  is useful in describing how the subsystem interconnects are made. In addition, this structure is very close to that of the actual block connects made with the Simulink block libraries. The vector  $u_1$  is an output from a previous component, and the output  $y_2$  provides feedback to the previous component. The output  $y_1$  supplies any subsequent blocks, and  $u_2$  allows for feedback from these blocks.

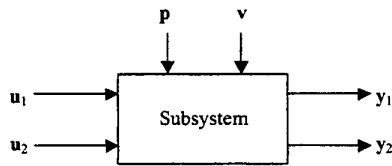


Fig. 3 Basic subsystem structure.

Three types of inputs to the system have been identified: inputs completely independent of system variables, those dependent on previous components, and those fed back from subsequent components. Two types of outputs include those feeding subsequent components, and those acting as feedback to previous components. The connection of two component blocks is shown explicitly in Fig. 4. Based on the input and output vectors, the first entry of the double index gives the subsystem number, and the second entry provides the input or output vector number with the convention of Fig. 3. This

diagram shows how the systems are cascaded to build complex systems. Although the figure demonstrates a series connection, parallel connections are also possible, through the use of algebraic operations to combine inputs.

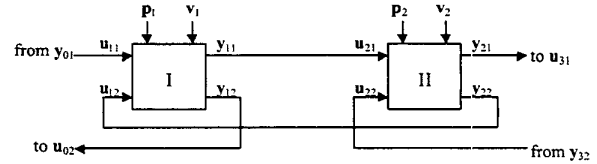


Fig. 4 Interconnection of multiple components.

The reason for the feedback paths can be understood in an intuitive way. Consider the simple example of a source with an attached load. When the source voltage is applied to the load, the current flow directly reflects upon the source, providing immediate feedback. In this simulation environment, the current must be calculated and fed back manually using an explicit signal line.

### IV. THE BLOCK LIBRARIES

A brief overview of the power electronic and machines blocksets is given here. The blocksets are set up as block libraries similar to the standard libraries that are provided with the package. The components are masked to provide an easy method for parameter setting by double-clicking to open a dialog window. By default, the blocks are initially locked, and cannot be modified. This default can be altered by manually breaking the library link. Then the internal structure of the blocks can be modified.

The power electronics blockset library is shown in Fig. 5.

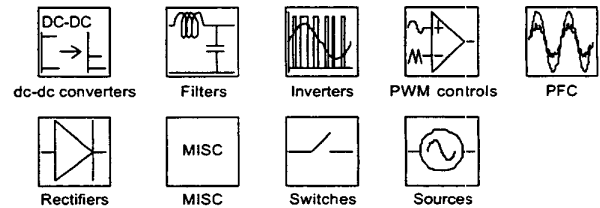


Fig. 5 Power electronics blockset library.

Each icon in the figure represents a suite of components, accessible by double-clicking. For example, opening the dc-dc converter suite provides the sub-library shown in Fig. 6.

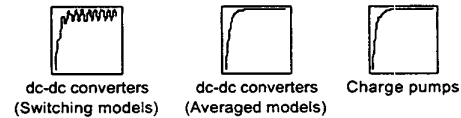


Fig. 6 The dc-dc converter suite

The dc-dc converter sub-libraries contain switching and averaged models with and without parasitic elements. The machines library is displayed in Fig. 7, which shows the dc, induction, synchronous, and permanent magnet machine blocksets.

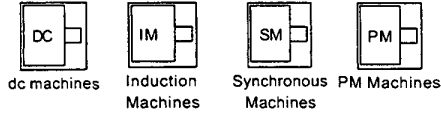


Fig. 7 Machines library.

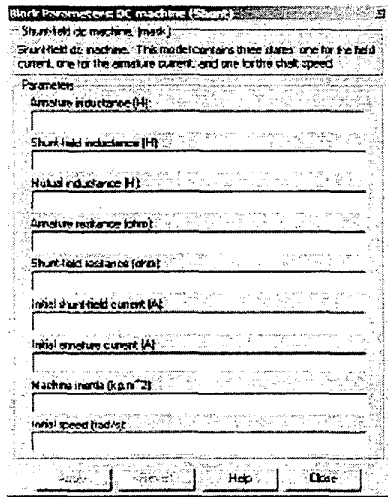


Fig. 8 Parameter window for the dynamic shunt-field dc machine model.

The parameters for each component can be set by double-clicking the component of interest. The resulting dialog for the dynamic shunt-field dc machine is shown in Fig. 8. The number of entries for the various components varies according to whether a dynamic or steady state model is used, whether or not a model with parasitic elements is used, and several other factors.

The integration routine used for system solution depends on the individual system being simulated. The solver type is selected from a global Simulink Parameters dialog. Even in the cases in which a variable-step solver can be utilized, for

validation purposes it is important to subject the system to a fixed-step routine, and then reduce the time step systematically to confirm the accuracy of the results.

## V. SIMULATION EXAMPLES

Two simulation examples will be considered in this section. Interconnection of the components to build complex systems will be examined in detail. The first example is a cascaded boost-buck power-factor-correction (PFC) regulated voltage supply. The second is a dynamometer example involving two coupled induction machines.

### A. Cascaded Boost-Buck PFC Regulated Supply

A two-stage boost-buck PFC regulated supply is considered in this section [10]. The front-end rectifier is a hysteretic controlled boost converter. The power stages are shown in Fig. 9. The input boost stage provides power factor correction, and the buck converter is used for voltage regulation at the load.

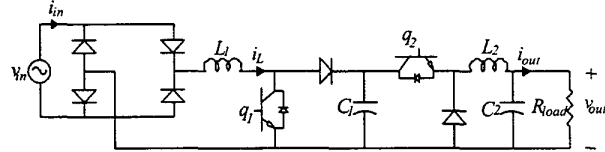


Fig. 9 Power stages for the cascade boost-buck PFC rectifier.

The block diagram for the system in the necessary form is given in Fig. 10. In this case, all switches are considered ideal. The front-end bridge is modeled by an absolute value block. The system utilizes two proportional-integral (PI) controllers, one to control the current magnitude for the PFC rectifier, the other to regulate the output voltage of the buck converter. The hysteretic controller forces the input current to follow a scaled version of the input voltage within certain error bounds by controlling the switch  $q_1$  as follows:

$$q_1 = \begin{cases} 1 & m|v_{in}| - i_L > \epsilon \\ q_1 & \epsilon \geq m|v_{in}| - i_L \geq -\epsilon \\ 0 & m|v_{in}| - i_L < -\epsilon \end{cases} \quad (9)$$

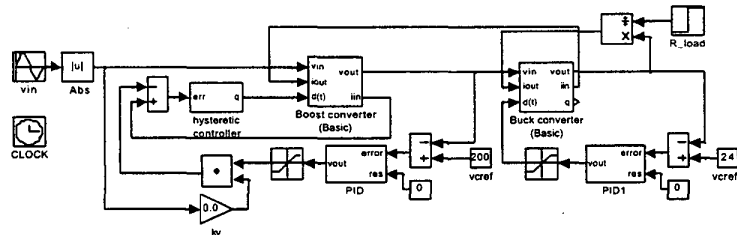


Fig. 10 Simulink block diagram for the cascade boost-buck power-factor-corrected rectifier with hysteretic controller.

From (9), the state of the switch  $q_i$  is selected to keep  $i_L$  in the interval  $[m|v_{in}| - \varepsilon, m|v_{in}| + \varepsilon]$ . If  $i_L$  is within these bounds, the switch state does not change. The scaling factor is provided directly from a PI controller whose input is the dc-link voltage error.

The simulation is performed with a fixed-step solver with a time-step of 1  $\mu$ s because the state-dependent hysteretic controller causes problems for a variable-step solver. The link voltage reference is 200 V, and the output voltage reference is 24 V. The load is initially 5  $\Omega$ , and at 0.3 s it is stepped to 2.5  $\Omega$ . The dc-link capacitor voltage and output voltage are displayed in Fig. 11. The input voltage, and the input current multiplied by a factor of 15 are shown in Fig. 12.

### B. Advanced Induction Machine Simulation

A coupled machine example is examined in this section. Both are symmetric three-phase induction machines [9], the first is a field-oriented-controlled (FOC) machine [14] with outer loop speed controller, and the second is direct-torque-controlled (DTC) [15]. The block diagram for the system is given in Fig. 13. The DTC machine acts as a dynamometer for the FOC machine. The Simulink block diagram for the system is displayed in Fig. 14 where the DTC machine is on the left, and the FOC machine is on the right.

The FOC machine uses an averaged model that neglects the switching frequency of the inverter. The DTC machine block models the inverter switching directly. For this example, the reference speed of the motor is regulated at 100 rad/s by a PI controller that provides the torque reference command to the FOC controller. At  $t=0$ , the reference torque to the dynamometer is 0.01 N·m, and at  $t=0.6$  s is increased to 10 N·m, and then to 30 N·m at 1.2 s. This is evident from the shaft speed plot of Fig. 15 in the dips and subsequent recoveries. The input power of the FOC machine, and the output power of the DTC dynamometer are shown in Fig. 16. The difference between the two curves represents the losses in the two machines. Finally, the shaft torque for both

machines is given in Fig. 17. Note that the developed torque for the DTC machine has significant ripple as compared to the FOC machine. This is usually the case for DTC drives because of the lower average switching frequency. As mentioned above, the FOC drive block is an averaged model, therefore torque ripple is not captured in the FOC inverter model.

## VI. CONCLUSION

A component library has been developed for use with Matlab/Simulink for the simulation of power electronic and machine systems. The toolboxes not only provide many components for simulation, but also introduce a systematic method for the construction of additional block components. The Simulink environment provides direct access to the computational ability of Matlab through a convenient, block diagram oriented programming environment.

The ability to model power electronic and machine systems in an expedient way is of value for both design and analysis. The block libraries also would be of benefit as teaching aids. Although the experience of building and testing real systems in a lab setting is indispensable for students studying machines and power electronics, a simulation tool such as the one presented offers students the ability to construct and test a myriad of virtual systems without the time and overhead associated with actual circuit construction. This potentially leads to a broader understanding of the operation of such systems.

## REFERENCES

- [1] The MathWorks, Inc., *Using Simulink, Version 2* Natick, MA: The MathWorks, 1997.
- [2] C. Ong, *Dynamic Simulation of Electric Machinery Using MATLAB/SIMULINK*. Upper Saddle River, NJ: Prentice Hall, 1998.
- [3] Sergey Lyshevski, *Electromechanical Systems, Electric Machines, and Applied Mechatronics*. Boca Raton, FL: CRC Press LLC, 2000.
- [4] A. Zuckerberger, D. Weinstock, A. Alexandrovitz, "Simulation of three-phase loaded matrix converter," *IEE Proc.-Electr. Power Appl.*, vol.143, no. 4, July 1996, pp. 294-300.

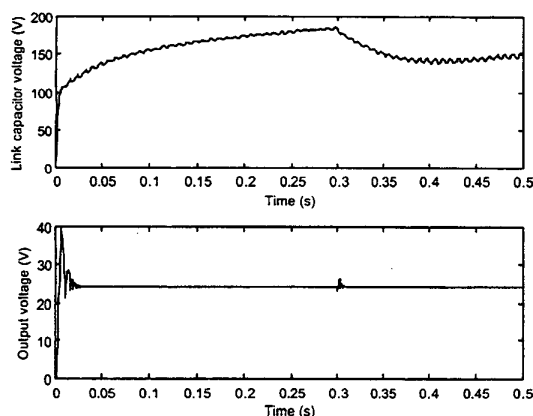


Fig. 11 PFC supply dc-link capacitor voltage and output voltage.

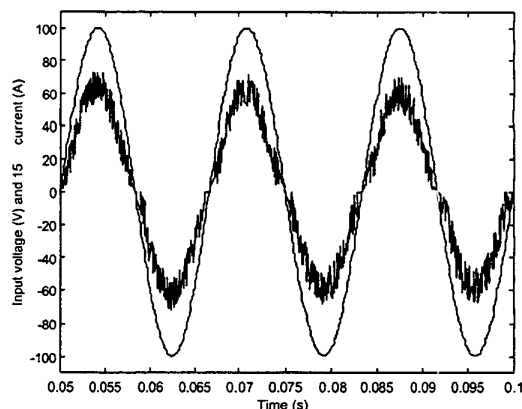


Fig. 12 Input voltage and current (current is multiplied by 15) for PFC supply.

- [5] B. Baha, "Modeling of resonant switched-mode converters using SIMULINK," *IEE Proc.-Electr. Power Appl.*, vol. 145, no. 3, May 1998, pp. 159-163.
- [6] S. Wade, et. al., "Modeling and simulation of induction machine vector control with rotor resistance identification," *IEEE Trans. Power Electronics*, vol. 12, no. 3, May 1997, pp. 495-506.
- [7] S. Ivanov, et. al., "Matlab-Simulink library for ac drives simulation," *International Conf. on SIMULATION*, Oct. 1998, pp. 195-200.
- [8] R. Teodorescu, "The development of a Simulink toolbox for advanced electrical drives simulation," *OPTIM 98*, pp. 573-576.
- [9] P. C. Krause, O. Wasynczuk, S. D. Sudhoff, *Analysis of Electric Machinery*. New York, NY: IEEE, 1995.
- [10] P. T. Krein, *Elements of Power Electronics*. New York: Oxford, 1998.
- [11] F. Tourkhani, et. al., "A variable-topology simulation tool for switchmode power supplies," *Proc. IEEE Int'l. Symp. Industrial Electronics*, 1999.
- [12] A. Nogueiras-Melendez, "A new complete non-linear simulation model of a buck dc-dc converter," *Proc. IEEE Int'l. Symp. Industrial Electronics*, 1999.
- [13] H. Jin, "Behavior-Mode Simulation of Power Electronic Circuits," *IEEE Trans. Power Electronics*, Vol. 12, No. 3, May 1997, pp. 443-452.
- [14] D. W. Novotny and T. A. Lipo, *Vector Control and Dynamics of AC Drives*. New York: Oxford, 1996.
- [15] P. Vas, *Sensorless Vector and Direct Torque Control*. New York: Oxford, 1998.

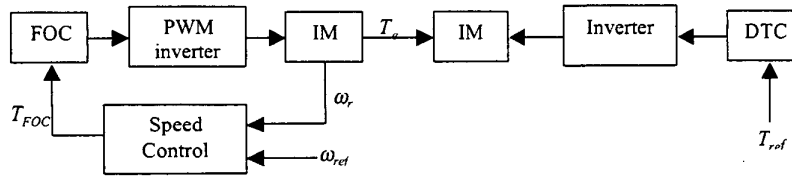


Fig. 13 FOC controlled induction machine with DTC controlled induction dynamometer.

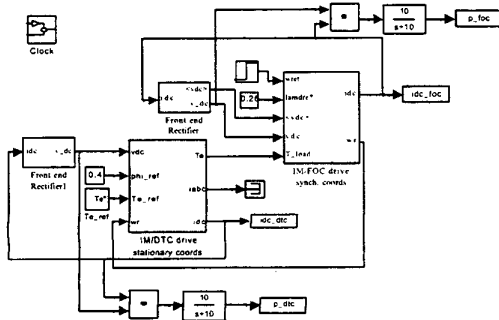


Fig. 14 Simulink block diagram for induction machine dynamometer example.

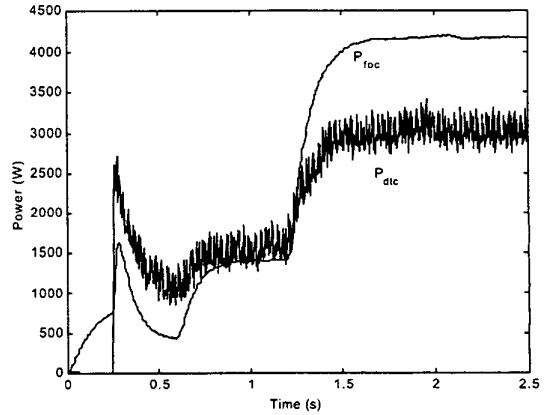


Fig. 16 Power out of FOC drive and into DTC drive.

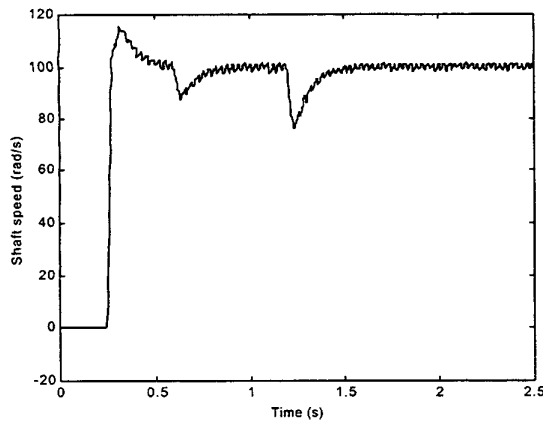


Fig. 15 Shaft speed of the induction machines for the dynamometer example.

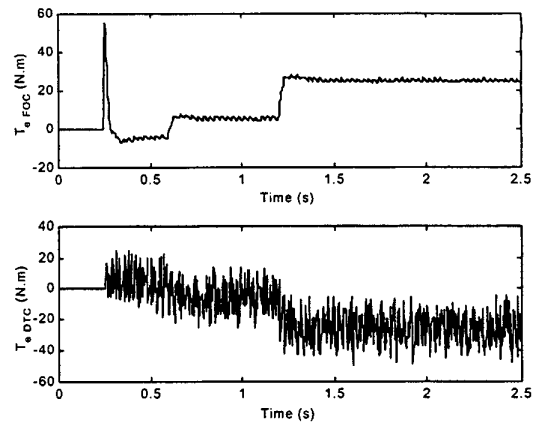


Fig. 17 Shaft torques for the FOC and DTC controlled machines.